Journal of the Chinese Society of Mechanical Engineers, Vol.47, No.2, pp 113~127 (2026)

Numerical Analysis of the Interaction between Two Adjacent Petrochemical Heaters under the Action of Strong Wind

Chun-Lang Yeh* and Qi-Ying Cai

Keywords：flow field interaction, relative position, computational fluid dynamics, stress analysis.

ABSTRACT

This study investigated the interaction of flow fields between two adjacent petrochemical heaters under the action of strong wind. The effect of flow field interaction on the force and stress distribution are analyzed for four relative positions of the two heaters. The analysis results reveal that the relative position of the heaters has a significant influence on the stress distribution. When the relative position of the two heaters changes, the pressure and vortex distribution through the heaters also change, and the pressure and friction forces acting on the heaters are affected, too. For heater A, when it is located behind heater B, heater A is subjected to the lowest stress and all monitored positions are safe without the risk of fatigue failure. When heater A is located to the right of heater B, heater A is subjected to the greatest stress and 23 of the 50 monitored stresses exceed the fatigue limit (75 MPa). On the other hand, for heater B, when heater A is located ahead of heater B (i.e., heater B is located behind heater A), the stress on heater B is the lowest and all monitored positions are safe without the risk of fatigue failure. When heater A is located to the right of heater B, heater B is subjected to the greatest stress and 9 of the 48 monitored stresses exceed the fatigue limit (75 MPa). When the smaller heater B is located behind the larger heater A, the pressure resistance of the rear heater B is smaller than that of the rear heater A when the larger heater A is located behind the smaller heater B. When heater A is located behind the right of heater B, the pressure resistance is greater than the case of one heater located behind or ahead of the other and less than the case of heater A located at the right of heater B. Further, when heater A is located behind the right of heater B, the stress on heater B is smaller than that on heater A.

Paper Received August, 2025. Revised January, 2026. Accepted February, 2026. Author for Correspondence: Chun-Lang Yeh.

* *Professor, Department of Aeronautical Engineering, National Formosa University, Yunlin, Taiwan 63208, ROC.*

INTRODUCTION

The structures of the heaters and stacks in a petrochemical industrial park are very close to the cylindrical structure, which often appears in the form of column groups. There is a strong aerodynamic interference among multi-cylindrical structures, which can easily cause wake excitation and even structural failure (Shen et al., 2012; Du, Zhang, and Liu, 2017). Therefore, the aerodynamic characteristics and interference effects of double cylinders have attracted much attention (Shen et al., 2012; Du, Zhang, and Liu, 2017; Zhou and Alam, 2016; Sumner, 2010; Zdravkovich, 1987). In the past, wind tunnel experimental methods were mainly used (Sumner, Richards, and Akosile, 2005; Ting, Wang, and Price, 1998; Alam, Sakamoto, and Zhou, 2005), but in recent years, computational fluid dynamics (CFD) have been increasingly used to study the interference problem among multiple cylinders.

Tahir et al. (2025) investigated the effect of gap spacing on wake transitions, hydrodynamic forces, and vortex synchronization phenomena around dual rectangular cylinders. A series of two-dimensional incompressible flow simulations was conducted using the Lattice Boltzmann method. The results highlighted a strong sensitivity of aerodynamic forces and vortex behavior to the transverse gap between rectangular cylinders. Proper tuning of gap spacing can mitigate flow-induced vibrations, reduce drag, and enhance thermal-fluid performance in engineering applications. Yin et al. (2024) investigated the two-dimensional vortex-induced vibration (VIV) of two side-by-side cylinders near a wall using the direct numerical simulation to reveal the VIV characteristics of the cylinders under the combined effects of the wall-cylinder interaction and cylinder-cylinder interaction. They examined four spacing ratios between the centers of two cylinders

and three gap ratios between the lower surface of the cylinder and the wall. The motion responses, fluid loads, vortex shedding frequencies, and wake modes are systematically analyzed. The results show that the lock-in regime of the reduced velocity depends on the spacing ratio. The wall effects suppress the transverse vibration and enhances the streamwise vibration of the cylinders, leading to a larger transverse amplitude on the upper cylinder and a larger streamwise amplitude on the lower cylinder. In addition, the wake patterns are sensitive to the gap ratio and spacing ratio, leading to abundant vortex shedding modes. Du et al. (2023) changed a circular cylinder to a square column to study its aerodynamic performance in a deflected flow. The authors focused on observing the time-frequency characteristics and span correlation of aerodynamics. Thiago, Jhon, and Carla (2022) used ANSYS CFX to simulate the turbulent flow field between adjacent cylinders. The authors explored the changes of drag coefficient and time trajectory of the cylinder at Reynolds numbers of 200, 1000 and 3000 with no change in the spacing ratio, and observed the vortex structure between the cylinders. Zhang et al. (2021) discussed the multi-cylinder system with unequal diameters commonly used in marine engineering. The authors used CFD to simulate two-dimensional double cylinders of unequal diameters under different spacing ratios to explore the interference effect. Grioni, Elaskar, and Mirasso (2020) discussed a higher subcritical Reynolds number ($Re=2\times10^5$) flow field. The authors changed the spacing ratio to explore the unsteady flow field around two cylinders. They also analyzed the gap effect between the cylinders through quantitative indicators such as the average/perturbation coefficient, pressure distribution, and wake structure behind the two cylinders. Fan et al. (2020) used particle image velocimetry and numerical simulation to explore the flow characteristics of two columns disturbed at high Reynolds numbers and different gap intervals. Wu, Sun, and Liu (2020) used wind tunnel test to study the relevant issues of aerodynamic interference characteristics of two columns at different spacing ratios. Zou et al. (2020) analyzed a staggered cone column with spacing ratios of 4 or 5 under the condition of Reynolds number Re=3900. They observed the lifting resistance characteristics, flow field structure and wake interference effect by changing the staggering angle from 0° to 15°. Ding et al. (2019) investigated the amplitude and frequency response of two square cylinders in fluid flow by changing their spacing and compared the results with the case of two circular cylinders. Eun et al. (2018) investigated the effect of positions of two cylinders perpendicular to parallel channels on the three-dimensional natural convection in the channel under the Reynolds numbers of $Re=10^4$~10^5. Wang, Mahbub Alam and Zhou (2018) placed larger cylinders in the wakes of smaller cylinders to observe the flow characteristics including flow structure, wake size, and eddy formation length. Liu et al. (2018) used 3D numerical simulations to explore the effect of changing the tilt angle on the flow characteristics behind two side-by-side cylinders under the condition of low Reynolds number (Re=100) and small spacing ratio. They analyzed the instantaneous and time-averaged flow fields, force coefficients, and Strouhal numbers. Du, Zhang, and Liu (2017) discussed the variation of the average drag, average lift, Strouhal number and flow structure of the parallel double cylinders with Reynolds number in the range of $Re=0.9\times10^5$~4.6×10^5. The authors also discussed possible interference factors. Zhou and Alam (2016) indicated that the interaction of airflow between two cylinders depends on the spacing between the two cylinders, the direction of fluid velocity and the Reynolds number. The authors discussed the physical mechanism of the airflow interaction between the two cylinders, including flow structure, heat transfer, and the momentum transport characteristics, etc.

In this paper, the flow characteristics and structural safety of two adjacent petrochemical heaters under the action of strong wind are analyzed. The numerical model and dimension of the two heaters are illustrated in Fig.1. Previous field monitoring result showed that the stacks of the two heaters have obvious oscillation under the action of northeast monsoon. In addition, visual and non-destructive inspection revealed that structural abnormalities have occurred in the two heaters, but one of the two heaters is damaged more seriously than the other. Why is there such a difference in the degree of damage for two adjacent heaters with similar size, structure, function and operating conditions? The oscillation of the heater is caused mainly by the airflow through the heater and the airflow pattern is closely connected with the relative positions of the two heaters. In this study, the flow and structure analysis of the two heaters is carried out to investigate the influence caused by the relative positions of the two heaters.

NUMERICAL METHODS

In this study, ANSYS FLUENT 2020 CFD software (ANSYS Inc., 2020) is used to simulate the flow field of the airflow through the two adjacent heaters. In terms of numerical models, Patankar's SIMPLE algorithm (Patankar, 1980) was used to solve the problem. In terms of the spatial discretization of the governing equations, the convection term is calculated by the power-law scheme and the diffusion term is calculated by the central difference scheme. In terms of physical models, the Reynolds number of the flow field discussed in this study is about $Re\approx2\times10^6$, which

falls in the range of high Reynolds number. According to the comments on turbulence models in relevant literature and the author's previous experience of simulating similar petrochemical equipment (Yeh, 2018; Yeh, 2021), the solution process of k-ε model is stable and for the high Reynolds number flow, the model together with the wall function method can generally obtain acceptable results, so the k-ε model is used in this study.

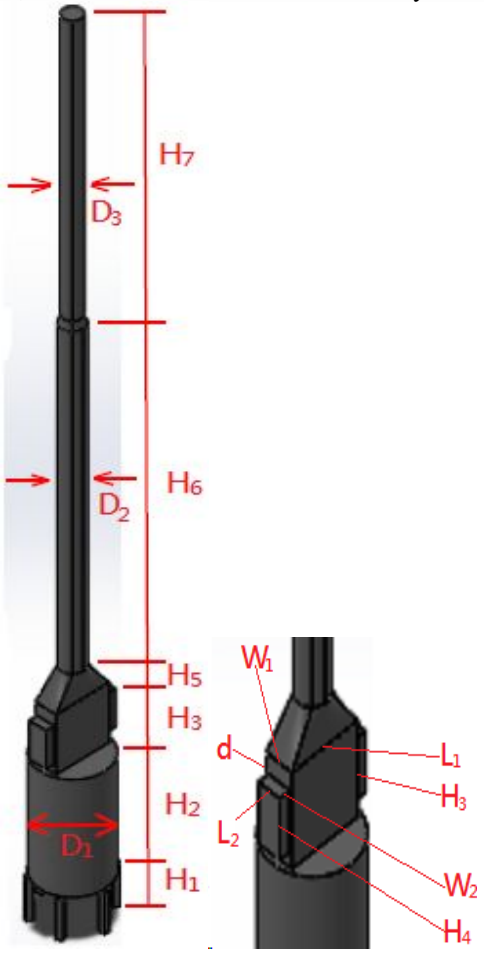

Unit: mm	Heater A	Heater B
H1	3048	3048
H2	8575	5667
H3	4655	4363
H4	2348	2348
H5	1601	1676
H6	32051	38941
H7	22047	23266
D1	4464	3985
D2	1572	1372
D3	1150	1191
W1	1772	2457
W2	500	557
L1	3850	3191
L2	856	856
d	1215	1089

(a) dimension of the two heaters

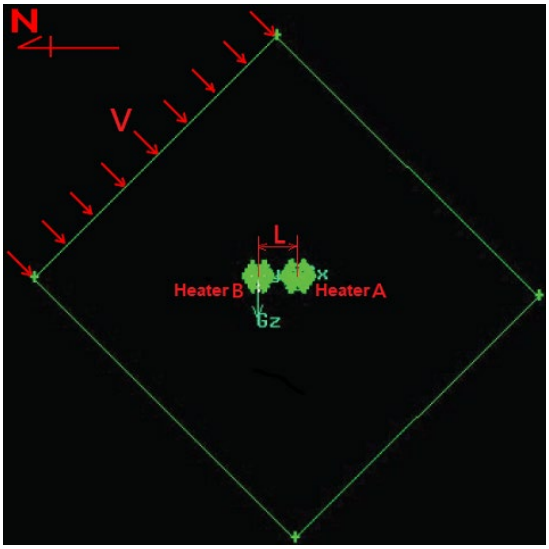

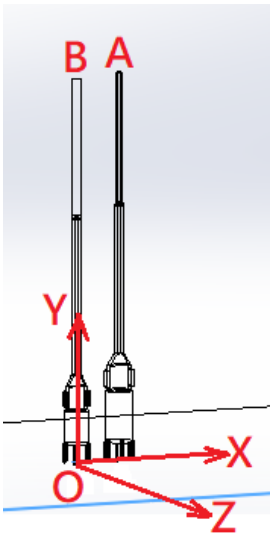

(b) illustration of the position of the two heaters (V：wind speed，L：distance between the two heaters；O：origin of the coordinate system (located at the bottom center of Heater B))

Fig. 1. Illustration of the geometry, dimension and position of the two heaters.

In terms of heater structure analysis, SOLIDWORKS 2020 software (Dassault Systèmes SolidWorks Corporation, 2020) was used to construct numerical model. Structure analysis is performed using ANSYS Workbench 2020R1 software (ANSYS Inc., 2020). The heater support frame is made of A-36 structural steel with a density of 0.284 lb/in^3. The inside of the stack is made of refractory mortar with a density of 0.046 lb/in^3. Young Modulus E and Ultimate Tensile Strength (UTS) σ_u are as follows:

Structural steel: $E=28.8\times10^6$ psi (199 GPa), $\sigma_u=58\times10^3$ psi (400 MPa);

Refractory mortar: $E=4.35\times10^6$ psi (30 GPa), $\sigma_u=725.19$ psi (5 MPa).

Structure analysis is widely used in structure

design, which can be divided into static analysis and dynamic analysis (modal analysis, harmonic response analysis, etc.). Static analysis is often used in structure engineering to calculate the displacement, stress, and strain of a structure under inertial forces (e.g., gravity, centrifugal force). Modal analysis is a method of studying the structure dynamics, which are the vibrational properties inherent in a system, each with its own specific natural frequency, vibration style, and damping ratio. Harmonic response analysis is used to determine the response of the structure to a time-varying sine wave (harmonic) load, which can be used to calculate the frequency response of the structure to the harmonic load, and to obtain the relationship between the response and frequency (Thomson, 2002) to verify whether the structure can overcome the resonance, fatigue and other harmful effects caused by vibration. The equations for static and dynamic analyses of a structure can be found in books on structure engineering and mechanics, e.g., (ANSYS Inc., 2020; Thomson, 2002).

RESULTS AND DISCUSSION

In this study, the flow and structure analysis of two adjacent heaters is carried out to understand the influence caused by the relative positions of the two heaters. Four relative positions of the two heaters are shown in Fig.2, in which the orientation of heater B relative to the wind direction is fixed, and four positions of heater A are studied. The position of heater A relative to the wind direction includes: (1) heater A 7.5m behind heater B, as shown in the case 1 of Fig.2, (2) heater A 7.5m ahead of heater B, as shown in the case 2 of Fig.2, (3) heater A 7.5m to the right of heater B, as shown in the case 3 of Fig.2, that is, the connection line of the two heaters is perpendicular to the wind direction, which means that the orientation of the two heaters relative to the wind direction are identical, (4) heater A 7.5m behind the right of heater B, as shown in the case 4 of Fig.2, which is the current status of the two heaters.

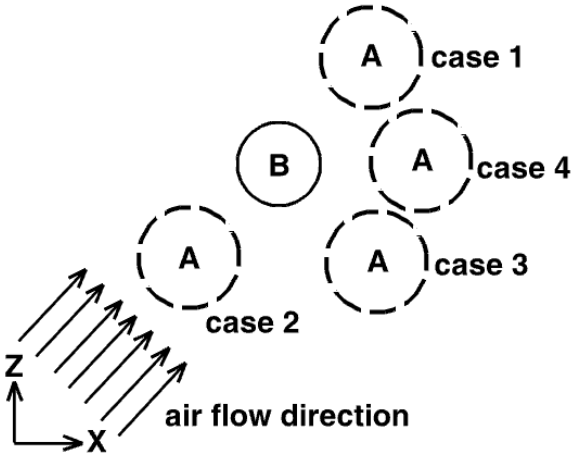

Fig. 2. Illustration of the relative positions of the two heaters.

Flow Analysis of the Two Heaters at Different Relative Positions

For the numerical model of flow analysis shown in Fig.1, six mesh densities are examined, including 1.51 million, 2.02 million, 2.51 million, 3.01 million, 3.51 million, and 4.02 million. The maximum computed gage pressures obtained using 3.51 million and 4.02 million unstructured meshes differ only by 1% and therefore the 3.51 million unstructured meshes is adopted for the CFD simulation. The maximum wind speed of 22 m/s measured in previous field monitoring of the two heaters is used in this study, and the Reynolds number based on this wind speed and the stack largest diameter of heater A is 2×10^6, which falls in the range of high Reynolds number. On the solid wall, the wall function method is used to consider the wall effect. At the free boundaries, the pressure is set as atmospheric pressure. The numerical methods for flow simulation used in this study have been successfully applied in the author's previous studies (Yeh, 2018; Yeh, 2021) for similar petrochemical equipment.

When the relative position of the two heaters changes, the distribution and strength of the velocity and vortex through the heaters will also change, and the pressure and friction forces acting on the heaters will be affected, too. Therefore, the relative position has a significant influence on the force distribution. When the fluid flows through a blunt body, the boundary layer is separated due to friction on the surface of the blunt body. A low-pressure and low-speed wake region is generated behind the blunt body, and two vortices are staggered on both sides of the blunt body and rotate in opposite directions. This results in a perturbation perpendicular to the flow direction, which causes the blunt body to vibrate. When the frequency of the vortex shedding is consistent with the natural frequency of the blunt body, resonation and serious structural damage of the blunt body will occur.

Fig. 3 to Fig. 6 show the distribution of pressure and vortex for airflow through the two heaters at y=2m, 6m, 13m, and 20m sections, respectively. At y=2m (Fig. 3), the two heaters are in the position of the six foundations, at y=6m (Fig. 4), both heaters are in the radiation section, at y=13m (Fig. 5), both heaters are in the convection section, and at y=20m (Fig. 6), both heaters are in the stack section. The resistance caused by the airflow through a heater mainly includes pressure resistance and friction resistance. The influence of the pressure resistance is more prominent than the friction resistance. The pressure resistance is closely related to the front high-pressure area and the rear wake area caused by the airflow through the heater. Because the average

diameter of heater A is larger than that of heater B, when heater A is located ahead of heater B, the high-pressure area ahead of heater A is larger than the high-pressure area ahead of heater B when heater B is located ahead of heater A. In addition, when heater A is located behind heater B, the wake area behind heater A is larger than the wake area behind heater B when heater B is located behind heater A. In terms of force, when heater B is located behind heater A, the difference between the range of the high-pressure area ahead of heater B and the wake area behind heater B is smaller, so the pressure difference across heater B is smaller. On the contrary, when heater A is located behind heater B, the difference between the range of the high-pressure area ahead of heater A and the wake area behind heater A is larger, so the pressure difference across heater A is larger. Therefore, the pressure resistance of the rear heater B when heater B is located behind heater A is smaller than the pressure resistance of the rear heater A when heater A is located behind heater B.

When heater A is located at the right of heater B, the two heaters are not behind or ahead of the other relative to the wind direction. The airflow between the two heaters accelerates due to the contraction effect, forming a low-pressure area, which is combined with the wake area behind the two heaters to form a larger low-pressure area. The high-pressure area ahead of the two heaters is also combined into a larger high-pressure area. Compared with the situation of one heater located behind or ahead of the other, the difference between the range of the high-pressure area ahead of the heaters and the wake area behind the heaters is larger when heater A is located at the right of heater B. Therefore, the pressure resistance is greater when heater A is located at the right of heater B in comparison with the situation of one heater located behind or ahead of the other.

When heater A is located behind the right of heater B (current status), the two heaters and the wind direction are at an angle of 45 degrees and the airflow between the two heaters is biased towards heater B and deviates from heater A, which causes the wake area behind heater A and the pressure difference across heater A to be larger. Therefore, the force on heater A is greater than that on heater B. Further observation reveals that when heater A is located behind the right of heater B, the difference between the range of the front high-pressure area and the rear wake area is greater than the case of one heater located behind or ahead of the other and less than the case of heater A located at the right of heater B. Therefore, the pressure resistance is also greater than the case of one heater located behind or ahead of the other and less than the case of heater A located at the right of heater B.

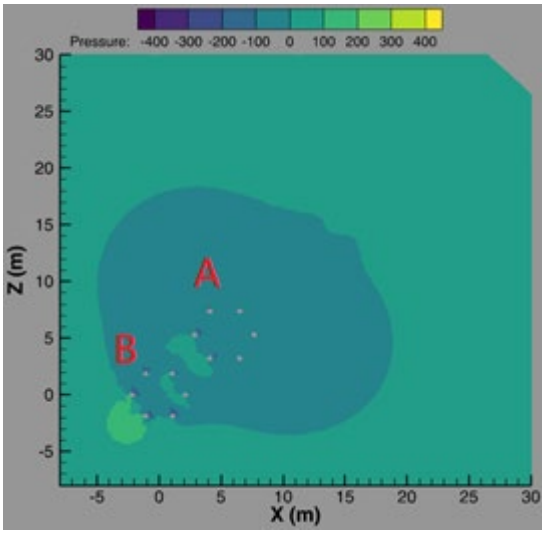

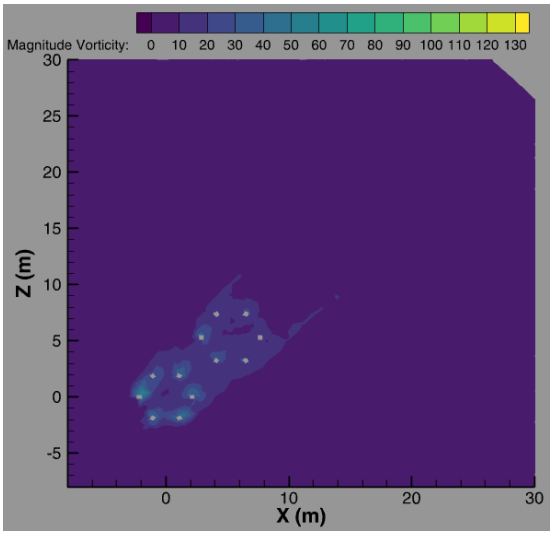

(a) heater A 7.5m behind heater B

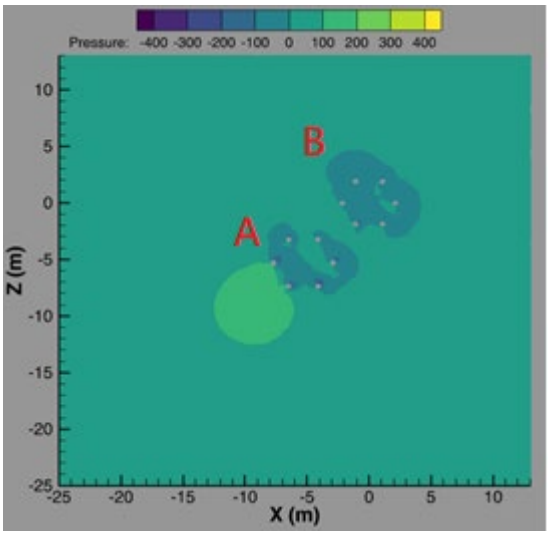

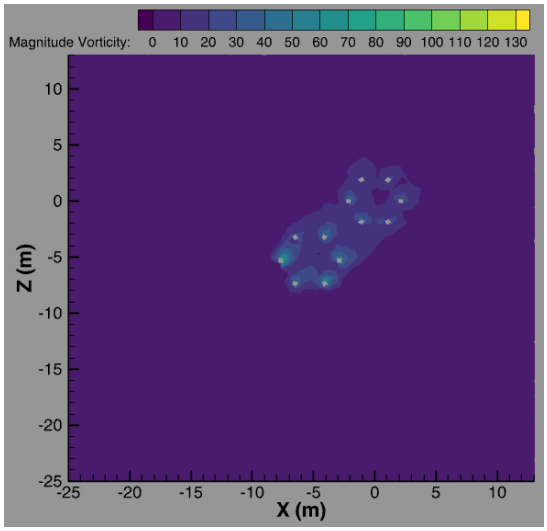

(b) heater A 7.5m ahead of heater B

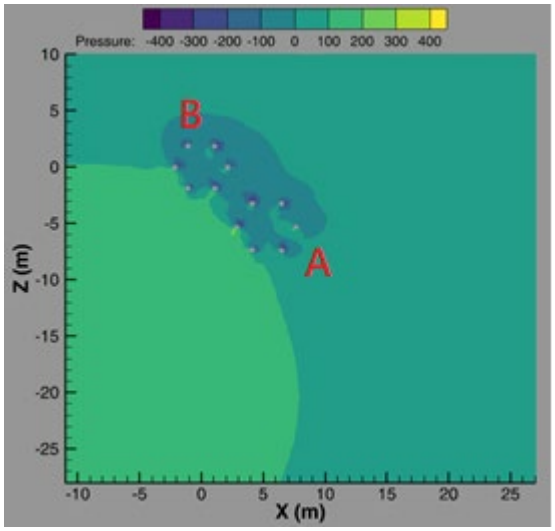

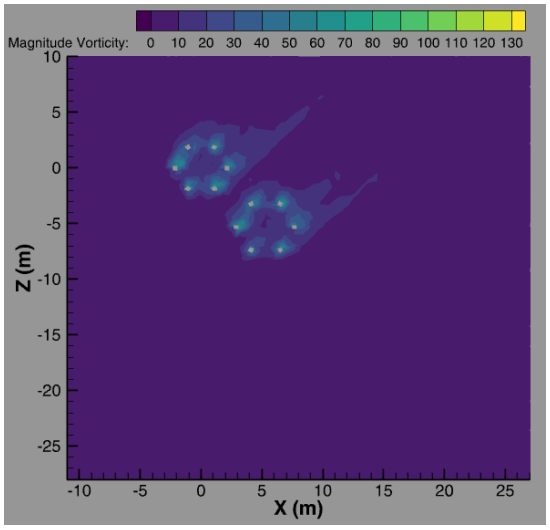

(c) heater A 7.5m to the right of heater B

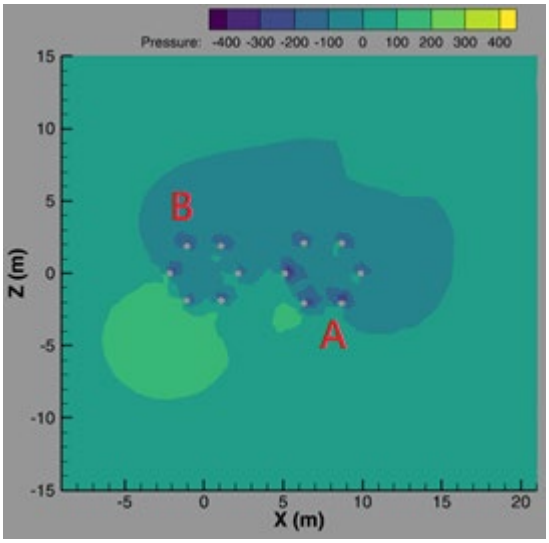

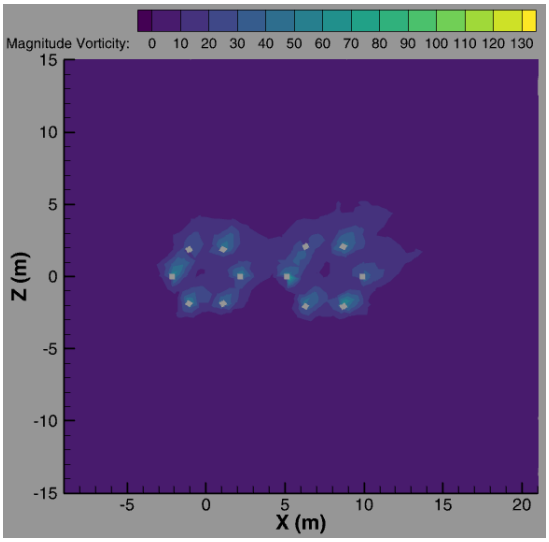

(d) heater A 7.5m behind the right of heater B

Fig. 3. Distribution of pressure (Pa) and vortex (sec^{-1}) for airflow through the two heaters at y=2m section.

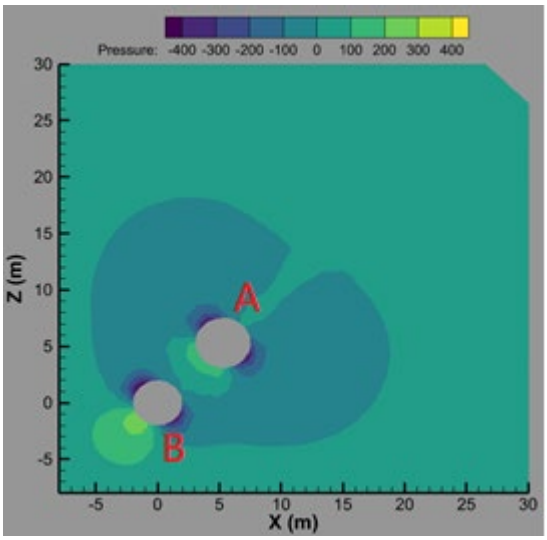

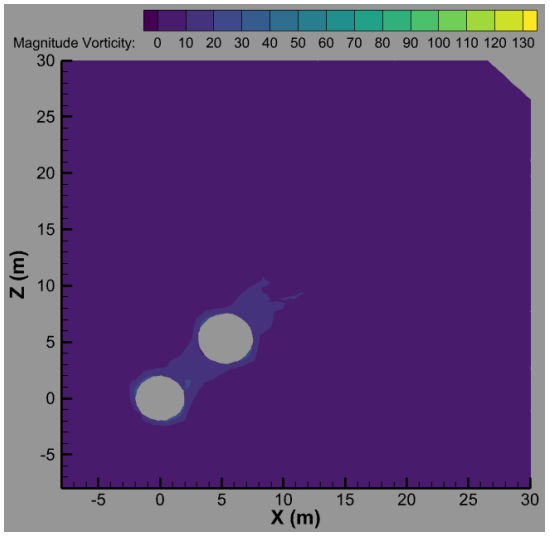

(a) heater A 7.5m behind heater B

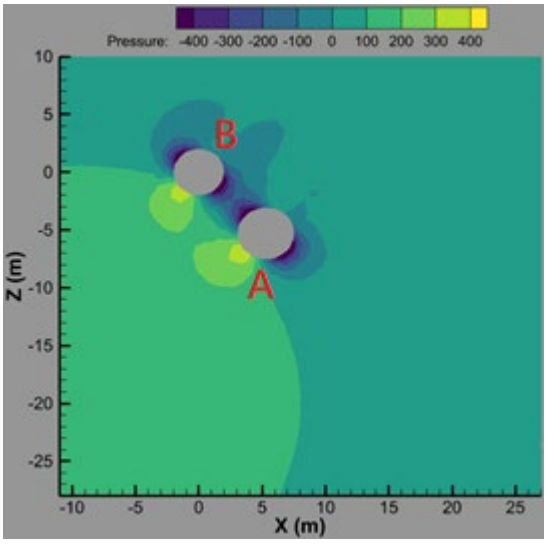

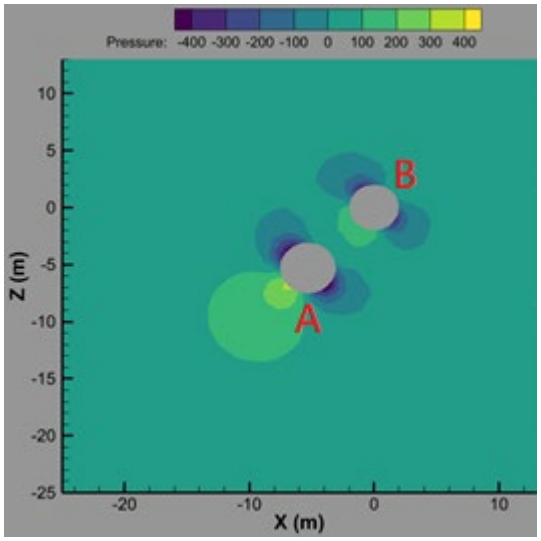

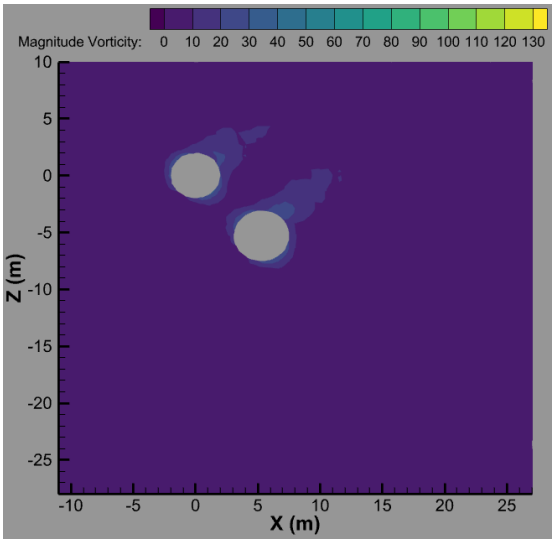

(c) heater A 7.5m to the right of heater B

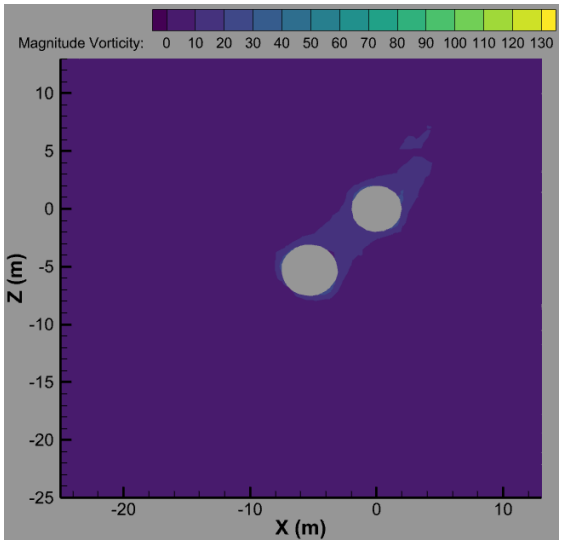

(b) heater A 7.5m ahead of heater B

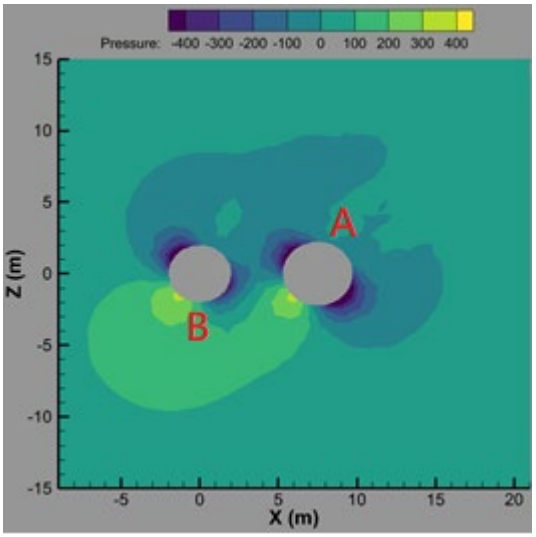

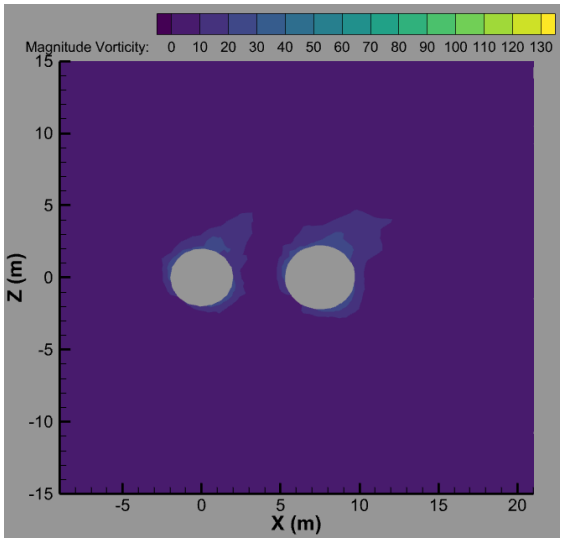

(d) heater A 7.5m behind the right of heater B

Fig. 4. Distribution of pressure (Pa) and vortex (sec^{-1}) for airflow through the two heaters at y=6m section.

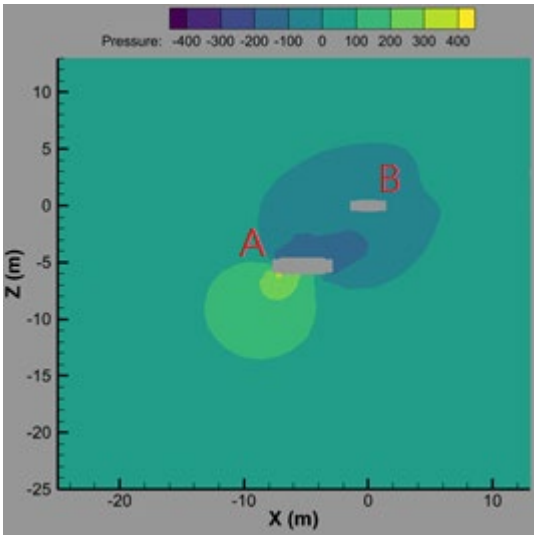

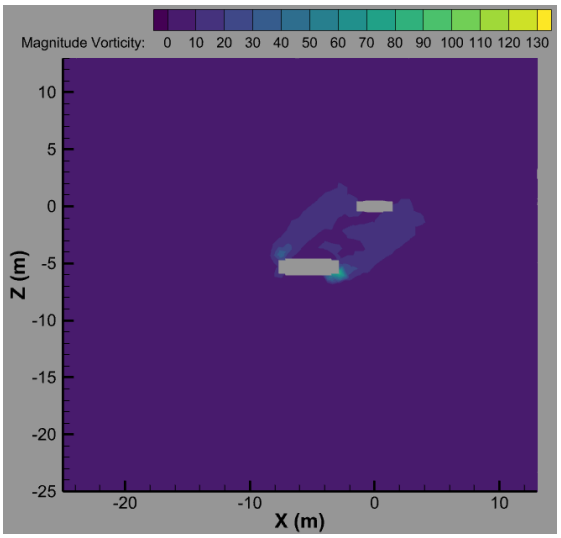

(b) heater A 7.5m ahead of heater B

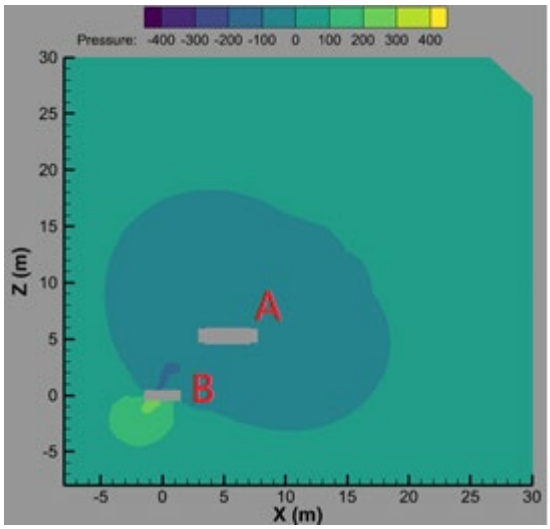

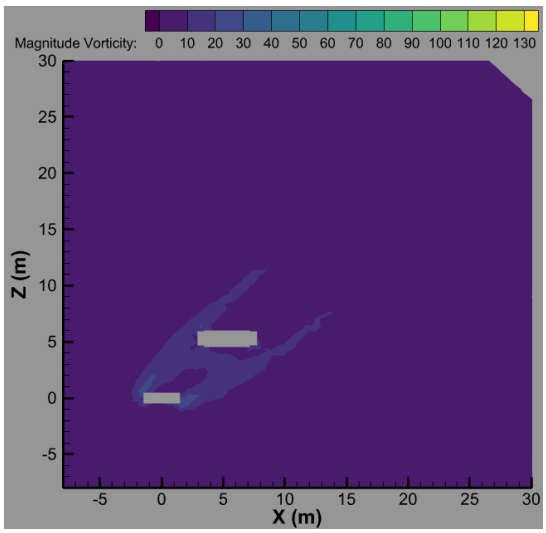

(a) heater A 7.5m behind heater B

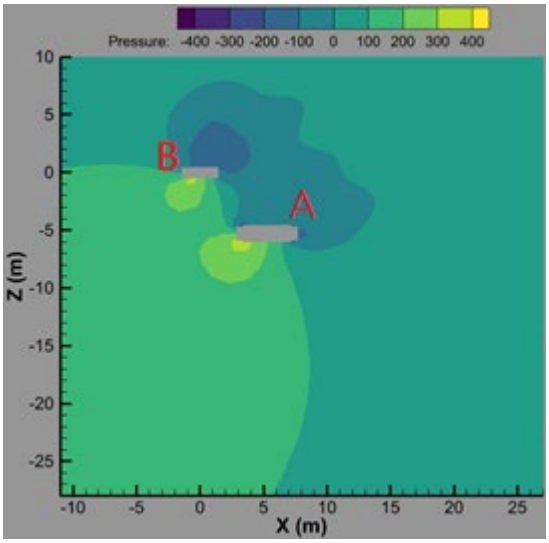

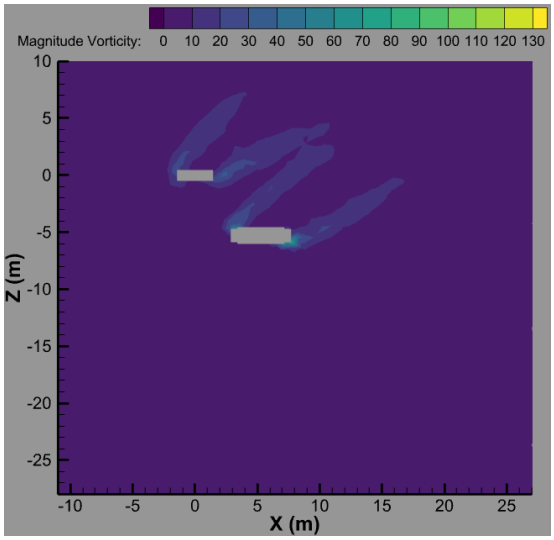

(c) heater A 7.5m to the right of heater B

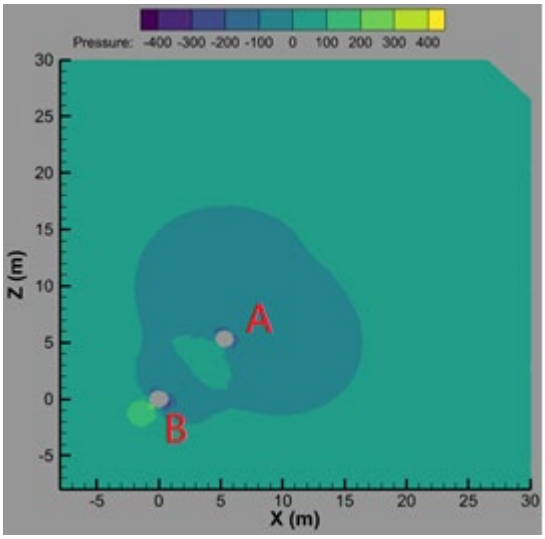

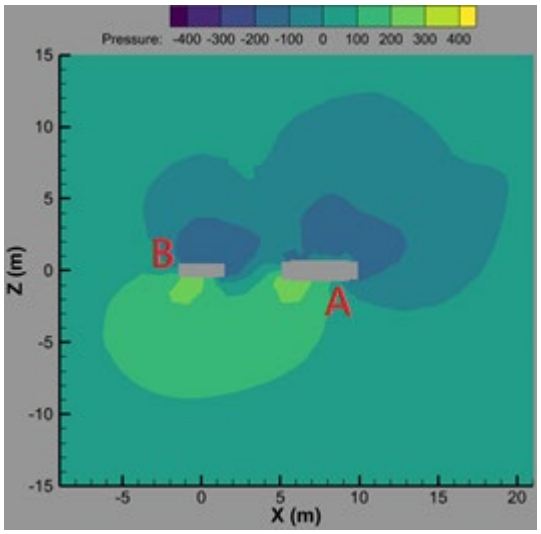

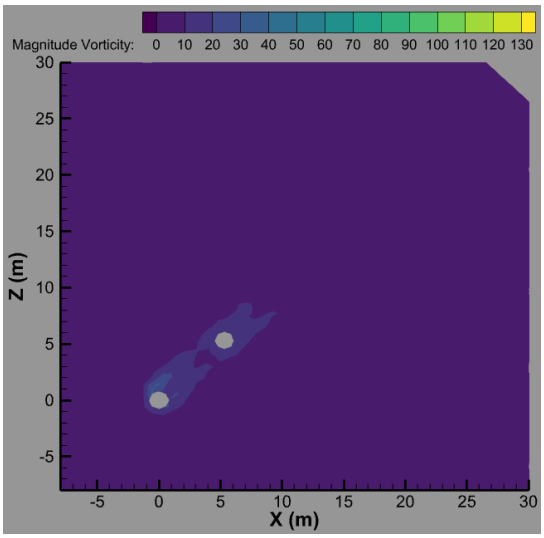

(a) heater A 7.5m behind heater B

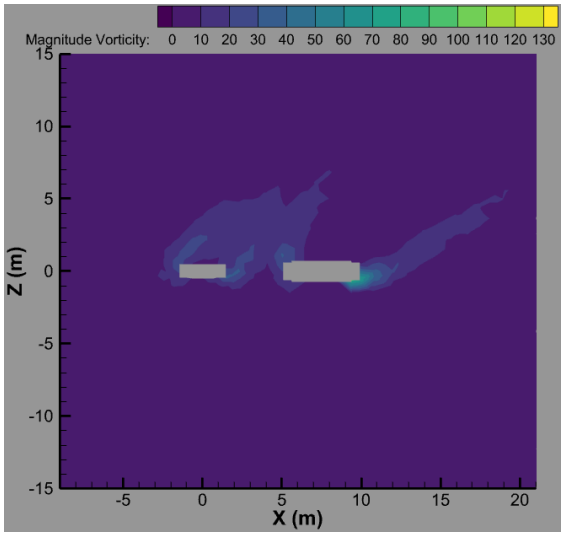

(d) Heater A 7.5m behind the right of heater B

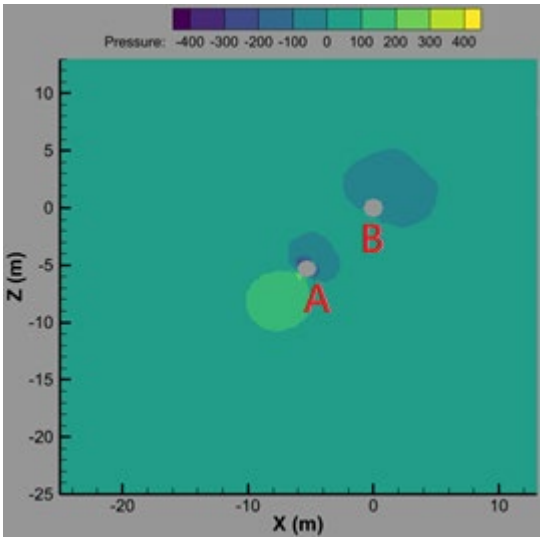

Fig. 5. Distribution of pressure (Pa) and vortex (sec^{-1}) for airflow through the two heaters at y=13m section.

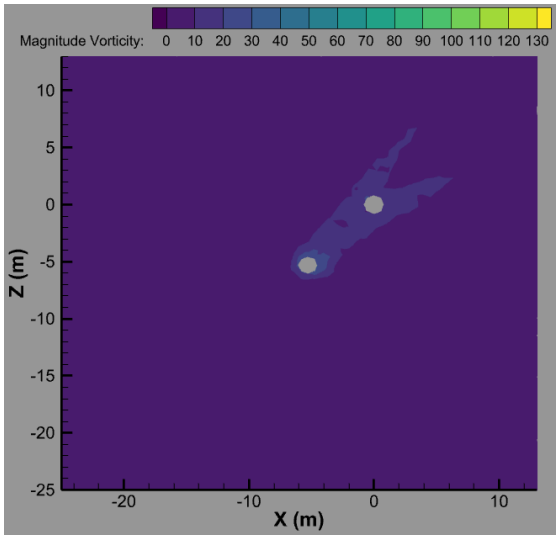

(b) heater A 7.5m ahead of heater B

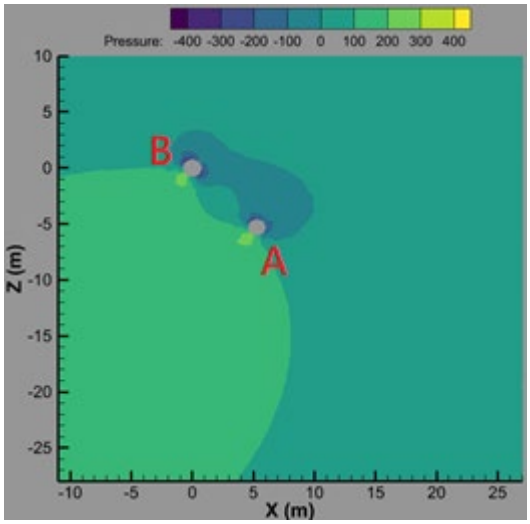

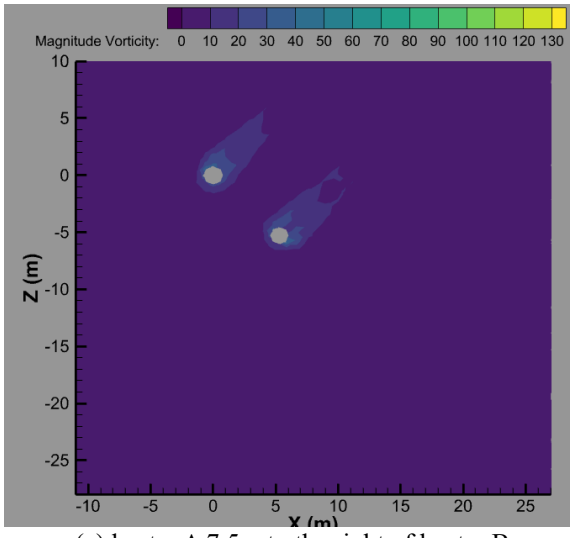

(c) heater A 7.5m to the right of heater B

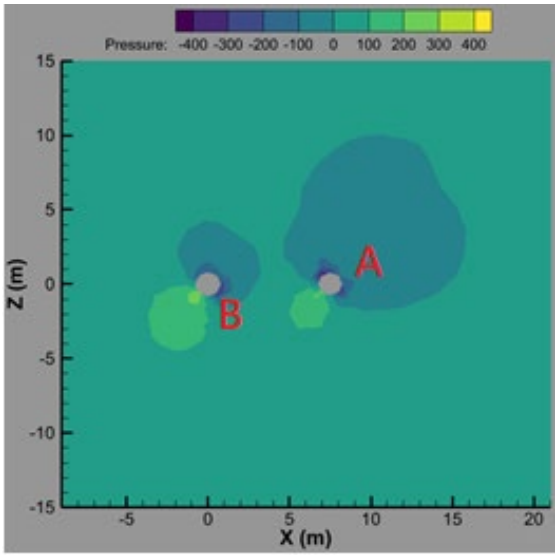

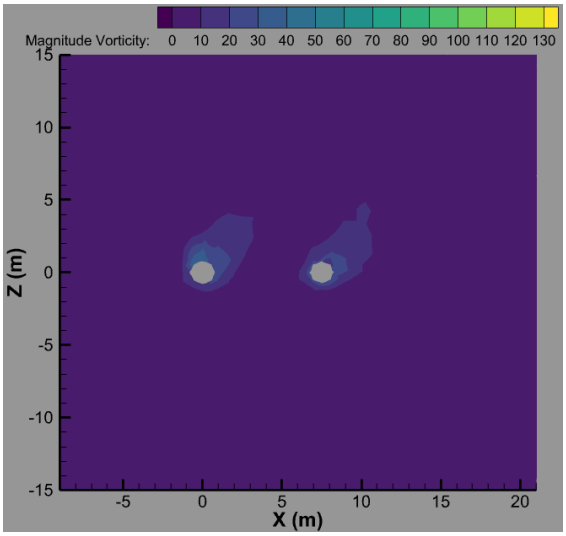

(d) heater A 7.5m behind the right of heater B

Fig. 6. Distribution of pressure (Pa) and vortex (sec^{-1}) for airflow through the two heaters at y=20m section.

Structure Analysis of the Two Heaters at Different Relative Positions

In order to confirm the results of the flow analysis, ANSYS MECHANICAL software was used to analyze the structure of the heaters. The numerical model is shown in Fig.7. The number of finite elements of the numerical model is about 6×10^5, which has been used in the author's previous study (Yeh, 2022) and is adequate for obtaining mesh-independent solution. In addition to the author's previous study (Yeh, 2022) and the present study, the stress analysis procedure in this study has also been applied successfully to similar petrochemical equipment in the author's previous study (Yeh and Chung, 2024). The maximum wind speed during stress monitoring of the two stacks in 2012 was 22 m/s, which is classified as a magnitude

9 wind speed according to the Beaufort wind scale. This wind speed corresponds to a mild typhoon.

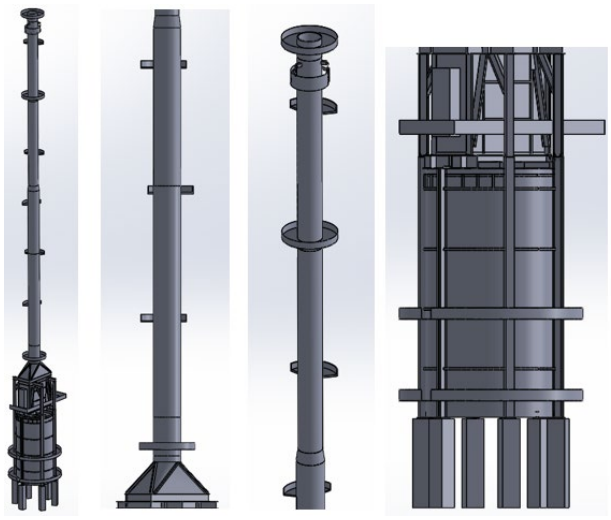

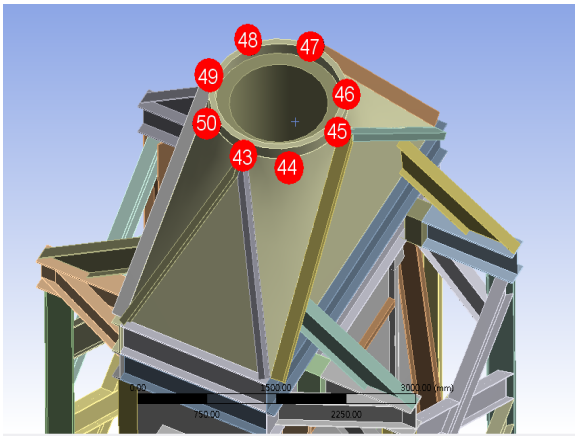

(a) heater A

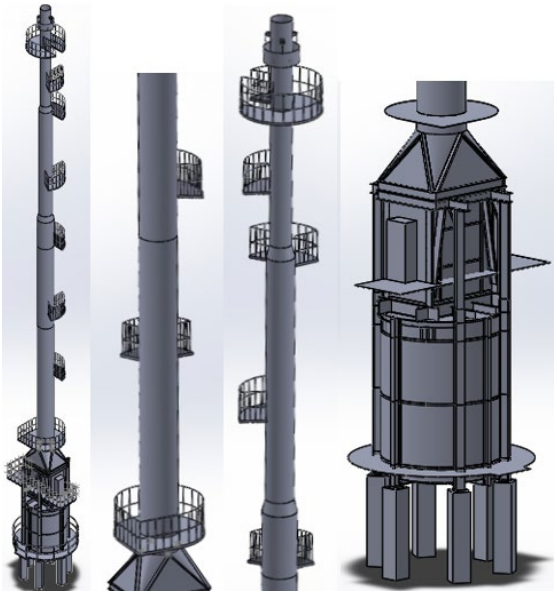

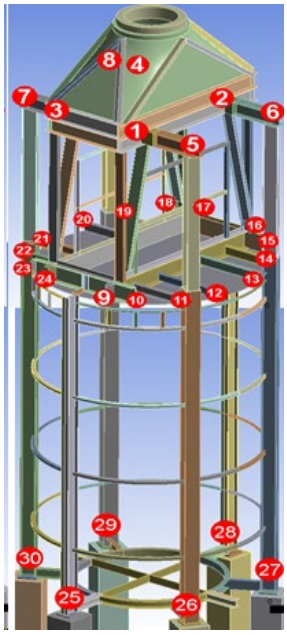

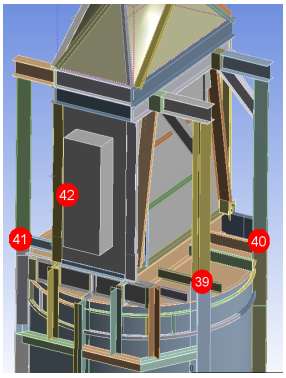

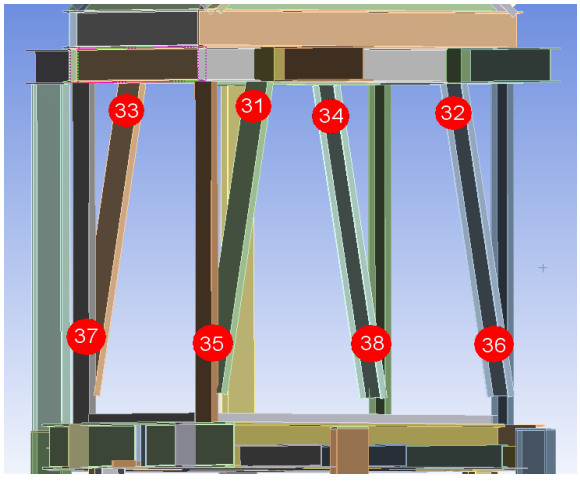

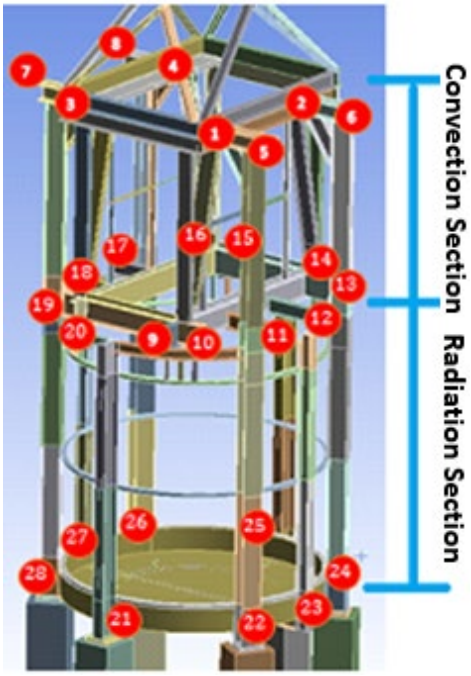

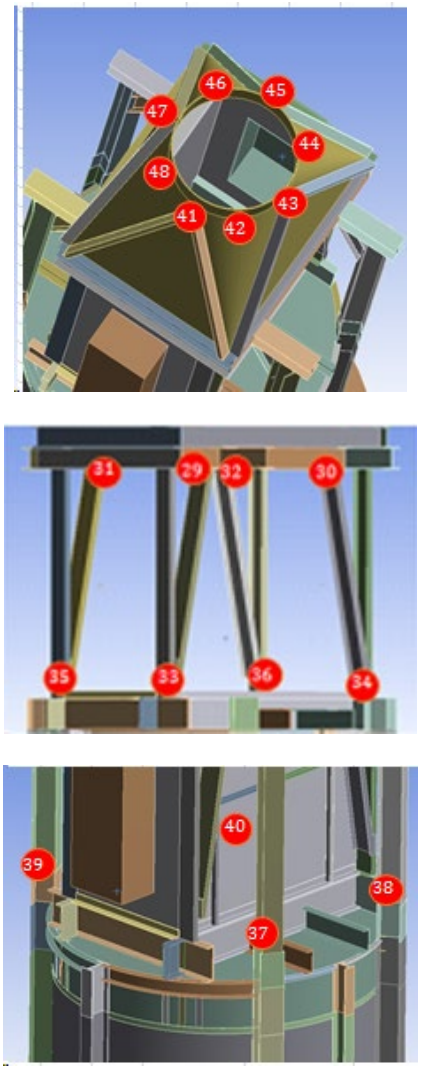

(b) heater B

Fig. 7. Heater structure model and illustration of the stress positions.

In this study, the ANSYS FLUENT software was used to analyze the flow field for the four relative positions shown in Fig.2 to find the forces on the two heaters at various relative positions, and then the forces on the two heaters were divided by their masses to obtain the individual accelerations of the two heaters in each relative position. The ANSYS MECHANICAL software was then used to solve the stress distribution of the two heaters based on the acceleration of the two heaters. The stress distribution of the two heaters in each relative position is shown in Table 1. From the analysis results, it can be observed that for heater A, when it is located behind heater B, heater A is subjected to the lowest stress and all monitored positions are safe without the risk of fatigue failure. When heater A is located to the right of heater B, heater A is subjected to the greatest stress and 23 of the 50 monitored stresses exceed the fatigue limit (75 MPa). On the other hand, for heater B, when heater A is located ahead of heater B (i.e., heater B is located behind heater A), the stress on heater B is the lowest and all monitored positions are safe without the risk of fatigue failure. When heater A is located to the right of heater B, heater B is subjected to the greatest stress and 9 of the 48 monitored stresses exceed the fatigue limit (75 MPa). When heater A is located behind the right of heater B (i.e., the current status), the stress is greater than the case of one heater located behind or ahead of the other and less than the case of heater A located at the right of heater B. Further, when heater A is located behind the right of heater B, the stress on heater B is smaller than that on heater A. This result can explain why the size, function, structure design and working conditions of the two heaters are similar, but the damage degree of heater A is more serious than that of heater B. The above stress analysis results are consistent with the flow analysis results.

Table 1. Stress distribution of the two heaters. (The stresses exceeding the fatigue limit (75 MPa) are marked in red.)

(a) heater A

Relative position	A 7.5m behind the right of B	A 7.5m behind B	A 7.5m to the right of B	A 7.5m ahead of B
Stress position	Stress (MPa)	Stress (MPa)	Stress (MPa)	Stress (MPa)
1	97.657	40.17	120.89	95.66
2	72.894	29.98	90.24	71.40
3	77.352	31.82	95.76	75.77
4	104.59	43.02	129.48	102.45
5	111.54	45.88	138.08	109.26
6	100.34	41.27	124.21	98.29
7	99.795	41.05	123.54	97.75
8	110.33	45.38	136.58	108.07
9	72.809	29.95	90.13	71.32
10	114.44	47.07	141.67	112.10
11	54.023	22.22	66.88	52.92
12	32.395	13.32	40.10	31.73
13	39.425	16.22	48.81	38.62
14	98.494	40.51	121.93	96.48
15	100.62	41.39	124.56	98.56
16	55.046	22.64	68.14	53.92

17	72.134	29.67	89.30	70.66
18	127.56	52.47	157.91	124.95
19	114.4	47.05	141.62	112.06
20	38.918	16.01	48.18	38.12
21	37.928	15.6	46.95	37.15
22	40.168	16.52	49.73	39.35
23	98.494	40.51	121.93	96.48
24	55.093	22.66	68.20	53.97
25	7.4831	3.08	9.26	7.33
26	28.31	11.64	35.05	27.73
27	16.039	6.6	19.86	15.71
28	6.1549	2.53	7.62	6.03
29	28.967	11.91	35.86	28.37
30	15.933	6.55	19.72	15.61
31	122.53	50.4	151.68	120.02
32	99.5	40.93	123.17	97.46
33	105.84	43.53	131.02	103.67
34	106.88	43.96	132.31	104.69
35	92.64	38.1	114.68	90.74
36	59.617	24.52	73.80	58.40
37	72.288	29.73	89.49	70.81
38	89.614	36.86	110.94	87.78
39	29.304	12.05	36.28	28.70
40	26.417	10.87	32.70	25.88
41	25.824	10.62	31.97	25.30
42	39.012	16.05	48.29	38.21
43	8.9101	3.66	11.03	8.73
44	17.582	7.23	21.77	17.22
45	31.245	12.85	38.68	30.61
46	13.028	5.36	16.13	12.76
47	6.2842	2.58	7.78	6.16
48	17.733	7.29	21.95	17.37
49	31.845	13.1	39.42	31.19
50	7.3136	3.01	9.05	7.16

(b) heater B

Relative position	A 7.5m behind the right of B	A 7.5m behind B	A 7.5m to the right of B	A 7.5m ahead of B
Stress position	Stress (MPa)	Stress (MPa)	Stress (MPa)	Stress (MPa)
1	39.06	35.44	40.15	13.86
2	34.78	31.55	35.74	12.34
3	34.97	31.72	35.94	12.41
4	46.02	41.75	47.30	16.33
5	57.76	52.40	59.36	20.50
6	68.35	62.01	70.25	24.26
7	55.61	50.45	57.16	19.74
8	50.39	45.71	51.79	17.88
9	77.82	70.59	79.98	27.62
10	99.44	90.21	102.20	35.29
11	4.78	4.34	4.92	1.70
12	3.93	3.57	4.04	1.39
13	92.29	83.72	94.86	32.75
14	59.97	54.41	61.64	21.28
15	71.15	64.55	73.13	25.25
16	97.05	88.04	99.74	34.44
17	5.63	5.10	5.78	2.00
18	5.22	4.73	5.36	1.85
19	87.05	78.97	89.47	30.89
20	54.91	49.82	56.44	19.49
21	6.08	5.51	6.25	2.16
22	13.88	12.60	14.27	4.93
23	8.30	7.53	8.53	2.94
24	11.89	10.79	12.22	4.22
25	5.99	5.43	6.15	2.12
26	14.10	12.79	14.49	5.00
27	8.48	7.69	8.71	3.01
28	11.84	10.74	12.17	4.20
29	209.77	190.30	215.60	74.45
30	180.76	163.98	185.78	64.15

31	165.51	150.15	170.11	58.74
32	181.25	164.43	186.29	64.33
33	55.97	50.78	57.53	19.87
34	52.50	47.62	53.96	18.63
35	51.08	46.34	52.50	18.13
36	55.69	50.52	57.24	19.77
37	34.11	30.94	35.06	12.11
38	38.64	35.05	39.71	13.71
39	41.24	37.41	42.39	14.64
40	52.45	47.58	53.91	18.62
41	12.56	11.39	12.91	4.46
42	15.98	14.49	16.42	5.67
43	14.68	13.32	15.09	5.21
44	13.72	12.45	14.11	4.87
45	11.65	10.57	11.98	4.14
46	14.58	13.23	14.99	5.17
47	14.57	13.21	14.97	5.17
48	13.02	11.81	13.38	4.62

CONCLUSIONS

In this paper, the interaction of flow fields between two adjacent heaters under the action of strong wind is analyzed. The influence of the flow interaction on the force and stress distribution are analyzed for four relative positions of the two heaters. The analysis results reveal that the relative position of the two heaters has a significant influence on the force and stress distribution. When the relative position of the two heaters changes, the pressure and vortex distribution through the heaters also change, and the forces acting on the heaters are affected, too. From the analysis results, the following three main findings are obtained:

1. For heater A, when it is located behind heater B, heater A is subjected to the lowest stress and all monitored positions are safe without the risk of fatigue failure. When heater A is located to the right of heater B, heater A is subjected to the greatest stress and 23 of the 50 monitored stresses exceed the fatigue limit (75 MPa). On the other hand, for heater B, when heater A is located ahead of heater B (i.e., heater B is located behind heater A), the stress on heater B is the lowest and all monitored positions are safe without the risk of fatigue failure. When heater A is located to the right of heater B, heater B is subjected to the greatest stress and 9 of the 48 monitored stresses exceed the fatigue limit (75 MPa).
2. When the smaller heater B is located behind the larger heater A, the pressure resistance of the rear heater B is smaller than that of the rear heater A when heater A is located behind heater B.
3. When heater A is located behind the right of heater B (i.e., the current status), the pressure resistance is greater than the case of one heater located behind or ahead of the other and less than the case of heater A located at the right of heater B. In addition, the stress on heater B is smaller than that on heater A.

In addition to the relative orientation of the two heaters, the distance between the heaters also has a significant impact on the interaction of the flow field and the distribution of force and stress on the heaters, which can be a future topic for such research.

Acknowledgments: The author is grateful to the Formosa Petrochemical Corporation in Taiwan for providing valuable data and constructive suggestions to this research during the execution of the industry-university cooperative research project under the contract 113AF-059.

REFERENCES

Alam, M.M., Sakamoto, H., and Zhou, Y. “Determination of Flow Configurations and Fluid Forces Acting on Two Staggered Circular Cylinders of Equal Diameter in Cross-Flow,”; *J. Fluids & Struct.*, Vol.21, No.4, pp.63–394 (2005).

ANSYS Inc., *ANSYS FLUENT 2020 R1 Theory Guide*, Fluent Inc., New York, NY, USA, March 9, 2020.

ANSYS Inc., Southpointe, 2600 Ansys Drive, Canonsburg, PA 15317, USA. Available online: https://www.ansys.com/products#t=ProductsTab&sort=relevancy&layout=card&f:@products=[Workbench] (accessed on 15 April 2022).

Dassault Systèmes SolidWorks Corporation, 175 Wyman Street, Waltham, MA 02451, USA. Available online: https://www.solidworks.com/support/resource-center (accessed on 15 April 2022).

Ding, L., Ye, Q.Y., Wang, H.B., Yun, Y.J., and Zhang, L., “Analysis of Flow-Induced Vibration Motion Characteristics of Two Columns with Different Spacing Tandems,”; *J. Vib. Eng.*, Vol.32, No.2, pp.331–339 (2019).

Eun, H.J., Seo, Y.M., Park, Y.G., and Ha, M.Y., “Effect of a Two Cylinder Vertical Location on the Three-Dimensional Natural Convection between a Parallel Channel,”; *Korean Soc. Mech. Eng.*, Vol.42, No.2, pp.91–99 (2018).

Du, X.Q., Chen, T.Y., Xu, H.L., and Ma, W.Y., “Aerodynamic Characteristics of Two

Side-by-Side Square Cylinders in Biased Flow Regime,"; *J. Hunan Univ*., Vol.50, No.1, pp.100–108 (2023).

Du, X.Q., Zhang, L.P., and Liu, Q.K., "Effect of Reynolds Number on Average Aerodynamic Characteristics of Parallel Cables in Cable-Supported Bridges,"; *Eng. Mech*., Vol.34, No.3, pp.189–196 (2017).

Fan, X.Y., Qin, H., Shang, J.M., and Hu, S., "Flow Mechanism Investigation on Interference Effect of Two Square Cylinders in Tandem Arrangement,"; *J. Vib. Shock*, Vol.39, No.8, pp.230–238 (2020).

Grioni, M., Elaskar, S.A., and Mirasso, A. E., "A Numerical Study of the Flow Interference between Two Circular Cylinders in Tandem by Scale-Adaptive Simulation Model,"; *J. Appl. Fluid Mech*., Vol.13, No.1, pp.169–183 (2020).

Gu, Z., and Sun, T., "On Interference between Two Circular Cylinders in Staggered Arrangement at High Subcritical Reynolds Numbers,"; *J. Wind Eng. Ind. Aerodyn*., Vol.80, No.3, pp.287–309 (1999).

Liu, C., Gao, Y.Y., Qu, X.C., Wang, B., and Zhang, B.F., "Numerical Simulation on Flow Past Two Side by Side Inclined Circular Cylinders at Low Reynolds Number,"; *China Ocean Eng*., Vol.33, No.3, pp.344–355 (2019).

Patankar, S.V., *Numerical Heat Transfer and Fluid Flows*, McGraw-Hill, New York (1980).

Shen, G.H., Wang, N.B., Lou, W.J., and Sun, B.N., "Analysis of Tower Shape Factor in the Collapse of the Ferrybridge Cooling Towers,"; *Eng. Mech.*, Vol.29, No.8, pp.123–128 (2012).

Sumner, D., "Two Circular Cylinders in Cross-Flow: A Review,"; *J. Fluids Struct*., Vol.26, No.6, pp.849–899 (2010).

Sumner, D., Richards, M.D., and Akosile, O.O., "Two Staggered Circular Cylinders of Equal Diameter in Cross-Flow,"; *J. Fluids Struct*., Vol.20, No.2, pp.255–276 (2005).

Tahir, N., Khan, N.Z., Abbasi, W.S., Ayaz, M., Ahmad, Z., and Alhmiedat T., "Numerical Investigation of Wake Dynamics and Flow Interference Effects on Fluid-Structure Interaction of Dual Side-by-Side Rectangular Cylinders: A Lattice Boltzmann Study,"; *RINENG*, Vol.28, 107578 (2025).

Thiago, G., Jhon, G., and Carla, A., "Hydrodynamic Characteristics of Two Side-by-Side Cylinders at a Pitch Ratio of 2 at Low Subcritical Reynolds Numbers,"; *Fluids*, Vol.7, No.9, 287 (2022).

Thomson, W.T., *Theory of Vibration with Applications*, 3rd ed., CBS Publishers & Distributors, New Delhi, India (2002).

Ting, S.K, Wang, D.J., and Price, S.J., "An Experimental Study on the Fluid Elastic Forces for Two Staggered Circular Cylinders in Cross-Flow,"; *J. Fluids Struct*., Vol.12, No.3, pp.259–294 (1998).

Wang, L.J., Mahbub Alam, M., and Zhou, Y., "Two Tandem Cylinders of Different Diameters in Cross-Flow: Effect of an Upstream Cylinder on Wake Dynamics,"; *J. Fluid Mech*., Vol.836, pp.5–42 (2018).

Wu, Q.Y., Sun, Y.S, and Liu, X.B., "Study on the Aerodynamic Interference Effect of Two Side-by-Side Square Cylinders,"; *Eng. Mech*., Vol.37, No.1, pp.265–269 (2020).

Yeh, C.L., "Numerical Investigation of the Effects of Steam Mole Fraction and the Inlet Velocity of Reforming Reactants on an Industrial-Scale Steam Methane Reformer,"; *Energies*, Vol.11, 2082 (2018).

Yeh, C.L., "Effect of Burner Operation on the Catalyst Tube Lifetime of a Steam Methane Reformer：A Numerical Study,"; *Appl. Sci.*, Vol.11, 231 (2021).

Yeh, C.L., "Reinforcement Design of the Support Frame of a Petrochemical Heater,"; *Appl. Sci.*, Vol.12, 5107 (2022).

Yeh, C.L., and Chung, Y.H., "Structure Analysis of the Fractionator Overhead Vapor Line of a Delayed Coker Unit,"; *Appl. Sci.*, Vol.14, 7193 (2024).

Yin, P., Xin, J., Shi, F., Li, Y., Liu, X., and Shu, L., "Numerical Study on Hydrodynamic Interaction Characteristics of Vortex-Induced Vibration of Two Side-by-Side Cylinders Near the Wall,"; *Ocean Eng*., Vol.308, 118305 (2024).

Zdravkovich, M.M., "The Effects of Interference between Circular Cylinders in Cross Flow,"; *J. Fluids Struct*., Vol.1, No.2, pp.239–261 (1987).

Zhang, Y.M., Luo, L., Chen, W., Lin, Y.S., and Chi, Q.J., "Numerical Simulation of Flow around Two Parallel Cylinders with Unequal Diameters,"; *Ship Sci. Tech*., Vol.43, No.5, pp.48–52 (2021).

Zhou, Y., and Alam, M.M., "Wake of Two Interacting Circular Cylinders: A Review,"; *Int. J. Heat Fluid Flow*, Vol.62, pp.510–537 (2016).

Zou, L., Liu, J., Wu, W.N., Yan, Y.L., and Wei, Y.Y., "Numerical Simulation of Flow around Two Staggered Three-Dimensional Wavy Conical Cylinders,"; *J. Harbin Inst. Tech*, Vol.54, No.1, pp.163–170 (2022).